

## Safety guarantee technologies of water pressure and water quality: a case study in secondary water supply for high-rise buildings

Dongsheng Wang<sup>a,\*</sup>, Fuchun Jiang<sup>b,§</sup>, Hongbin Liu<sup>c</sup>, Hao Xiang<sup>a,d</sup>

<sup>a</sup>School of Automation and School of Artificial Intelligence, Nanjing University of Posts and Telecommunications, Nanjing 210023, China, Tel. +8618913939776; email: wdsnjupt@163.com (D. Wang)

<sup>b</sup>Suzhou Tap Co., Suzhou 215002, China, Tel. +8618115607225; email: 394799134@qq.com (F. Jiang)

<sup>c</sup>Co-Innovation Center of Efficient Processing and Utilization of Forest Resources, Nanjing Forestry University, Nanjing 210037, China, Tel. +862585427620; email: hongbinliu@njfu.edu.cn (H. Liu)

<sup>d</sup>Jiangsu Engineering Lab for IOT Intelligent Robots, Nanjing University of Posts and Telecommunications, Nanjing 210023, China, Tel. +8618260031022; email: nanjingxianghao@163.com (H. Xiang)

Received 27 May 2019; Accepted 14 December 2019

### ABSTRACT

With the rapid development of high-rise buildings in the past decades, the secondary water supply (SWS) has drawn great attention. In the traditional SWS of high-rise buildings, water pressure in the main pipeline is not enough to transmit water to high-rise rooftops, and thus water needs to be pumped to the rooftop water tank, then distributed to households with the help of gravity. Meanwhile, the water bio-indices assessment exceeds risk standards for the breeding of microorganisms and pathogens in rooftop water tanks. To avoid this phenomenon, the water pressure is boosted through an anti-negative pressure facility, and then water is distributed to households directly in the practical case of this work. Moreover, secondary disinfection, in which physical (ultraviolet) and chemical (sodium hypochlorite) disinfection techniques are combined, is implemented before the water enters occupants' homes. In this work, safety guarantee technologies of water pressure and water quality are successfully applied in a residential district of Suzhou, China. The results show that the qualified rate of water quality increases from 61% to 100%, and the water pressure fluctuates within 0.03 MPa.

*Keywords:* Anti-negative pressure facility; Ultraviolet; Sodium hypochlorite; Secondary water supply

### 1. Introduction

High-rise buildings have undergone considerable development over the past decades [1]. Compared with low-rise buildings, secondary water supply (SWS) of high-rise buildings require special attention [2]. Usually, the water pressure of the main pipeline is limited to a certain range to minimize the leakage rate in the water supply and to avoid bursting water mains. It is difficult to maintain a normal water supply for high-rise buildings because the water pressure

of pipelines is set at a relatively low level [3]. Therefore, the water of main pipeline must be pumped to the rooftop water tank of high-rise and then gravitationally distributed to households [4].

The anti-negative pressure facility (ANPF) provides a revolutionary solution for taking full advantage of the surplus pressure of main pipeline [5]. For directly pumping water from main pipeline to households by using a variable frequency pump, ANPF is adopted for the water supply of constant pressure and the negative pressure of main pipeline

\* Corresponding author.

§This author contributed equally to this work.

is eliminated. Thus, the safety of water pressure is guaranteed [6]. In addition, the rooftop water tank is replaced and the secondary pollution from external contaminants is avoided.

The safety of water quality is another vital problem in SWS [7–9]. During the long-distance transmission of water, complex physical, chemical and biological reactions lead to the growth of microorganisms and pathogens [10]. There are a few disinfectant residuals left for decay and consumption [11]. Thus, the water quality of SWS cannot be effectively guaranteed.

Chlorine is the most commonly used disinfectant, particularly for microbial growth control in drinking water distribution systems [12]. Chlorination suffers from the formation of disinfection by-products which may increase toxicity for humans, particularly at prolonged exposure times [13,14]. Sodium hypochlorite (NaClO) disinfection, in contrast, does not release free chlorine into water [15]. Thus, the formation of disinfection by-products is reduced [12,16]. As a method of physical disinfection, ultraviolet (UV) has been widely used for drinking water treatment over the past several decades for its high efficiency in inactivating pathogenic microorganisms and degrading emerging contaminants [17,18]. But the effectiveness of UV disinfection drops significantly in the case of high biomass concentration, as UV irradiation is affected adversely by water turbidity [19]. Thus, a composite secondary disinfection method consisting of NaClO and UV is an appropriate choice for guaranteeing the safety of water quality.

The major contribution of this work is the development of anti-negative pressure technology and composite disinfection technology for the SWS of high-rise buildings. The water pressure-driven method, anti-negative pressure technology, terminal disinfection technology, and integrating intelligence water management are introduced in Section 2. An optimization scheme of anti-negative pressure technology and a monitoring scheme of water bio-indices stability are proposed in Section 3. To date, this work has been successfully applied in the SWS of high-rise buildings of Suzhou, China.

## 2. Methods

### 2.1. Water pressure-driven method

In this work, the water pressure-driven method is used for hydraulic simulation. The traditional microscopic hydraulic model is difficult to simulate the changes in water pressure of main pipeline and node. During the simulations of MATLAB and EPANET, the node information is made closer to the actual water supply. The water flow of a node is adjusted to satisfy the following relationships:

- Conservation of water flow and the energy in gradient algorithm of EPANET.
- Relationship between water flow and water pressure in setting of MATLAB.

The method's core procedure is as follows:

- Capacity of water supply is calculated.
- Water flow  $D$  of a node is calculated under the formula [20].
- Updated water flow  $D_i$  of a node is obtained under the presetting conditions.

- Pipeline network is recalculated after the water flow of node is updated.
- Repeat steps ii–iv until the variance between  $D_i$  and  $D$  is within a certain precision.

### 2.2. Anti-negative pressure technology

The applicability of ANPF is analyzed through modifying the nodes' water consumption and the diameter, length, and pressure of main pipeline and access pipeline. The effect of superimposed water supply on the main pipeline is also developed under different water supply conditions. The research steps are as follows:

- Some pipeline network information, including the diameter, length and friction coefficient for the status of pipeline 1 and pipeline 2, and the elevation and rated water requirement of node 2, node 3 and node 4, is initially set up.
- Actual water allocation and water pressure of each node are obtained through changing the rated water demand of node 2 and simulating with the water pressure-driven method.
- Rated water demand of node 2 is gradually increased until the water pressure of node 2 within a certain limit.

Fig. 1 shows the programming flowchart of ANPF analysis. The pipeline network information includes the diameter, length, friction coefficient of pipeline 1 and pipeline 2, and the elevation and rated water demand of node 2, node 3 and node 4. The  $m$  denotes the increment of water flow of node 2,  $D_2$  denotes the water flow of node 2,  $P_2$  denotes the pressure of node 2 and  $\varepsilon$  denotes the certain limit.

The regional simulation of ANPF is shown in Fig. 2. A new node 2 is added at one point in the pipeline network. This node 2 connects pipeline 1 and pipeline 2 to node 3 and node 4, respectively. Given the water flow, water intake method and main pipeline characteristics of normal operation status, the diameter and length of pipeline 1 and pipeline 2, the flow and elevation of node 2, and the elevation of node 3 and node 4 are modified. The water pressure of node 2, node 3, and node 4 are analyzed by introducing different pipeline lengths and diameters while water flow changes in node 2.

### 2.3. Terminal disinfection technology

At present, SWS disinfection mainly depends on physical methods, such as heating, ultrasonic, UV, membrane, and high-voltage electrostatic. Considering the maturity of technology and the feasibility of disinfection, this work mainly discusses the UV and NaClO disinfection. Secondary disinfection facilities are installed at the outlet of a water tank. By introducing a reliable UV disinfection sterilizer and combining with NaClO, water quality is guaranteed.

Considering the requirement of real-time monitoring for SWS water-quality, the adenosine triphosphate (ATP) of water sample is analyzed in this work. The experimental content is as follows:

- Relation between the ATP and bacterial colonies.
- Disinfection effects of different UV intensity and UV-NaClO, and the capacity of bacteria regrowth after disinfection.

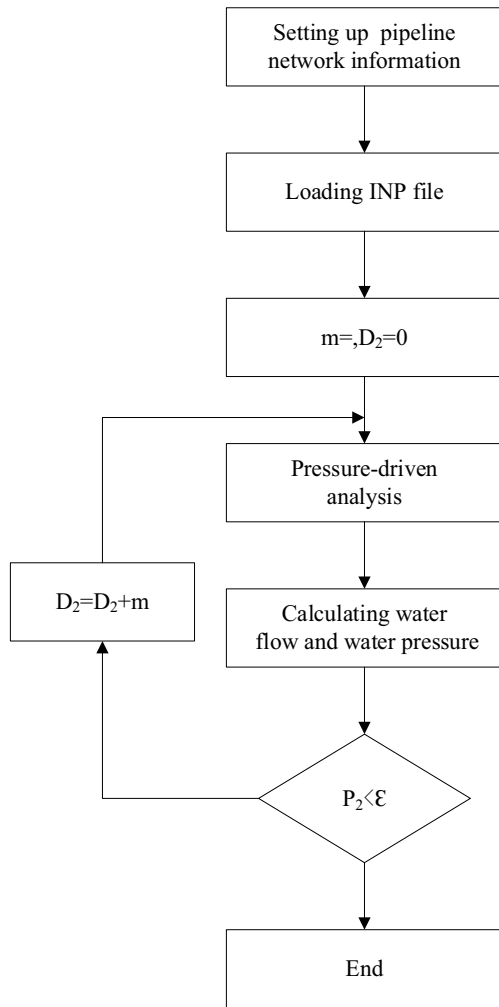


Fig. 1. Programming flowchart of ANPF analysis.

- Disinfection effects of UV for polluted tap water.
- Kinetics of bacterial growth in raw water and UV disinfection water with the dilution cultivation method.

The ATP is measured on ATP tester (BacTiter-Glo Alcohol, Promega Company, Madison, Wisconsin, USA). The 24 tap water samples are collected at a normal temperature within each hour of a day. After inoculating the nutrient solution of acetic acid carbon with the drinking water bacteria, the liquid is obtained in 6 d, and the ATP (relative light unit (RLU)) of bacterial liquid of 20, 30, 40, 50, 70 and 90  $\mu\text{L}$  are determined respectively. Fig. 3 shows the ATP of water sample.

2.4. Integrating intelligent water management

The concept of smart water is proposed based on IBM's smart planet. The smart water of this work indicates that the real-time perception of SWS operating status is conducted through data acquisition and transmission. Then, integrating management software makes SWS operation more reliable and intelligent. Fig. 4 shows the constitution of integrating intelligence water management software.

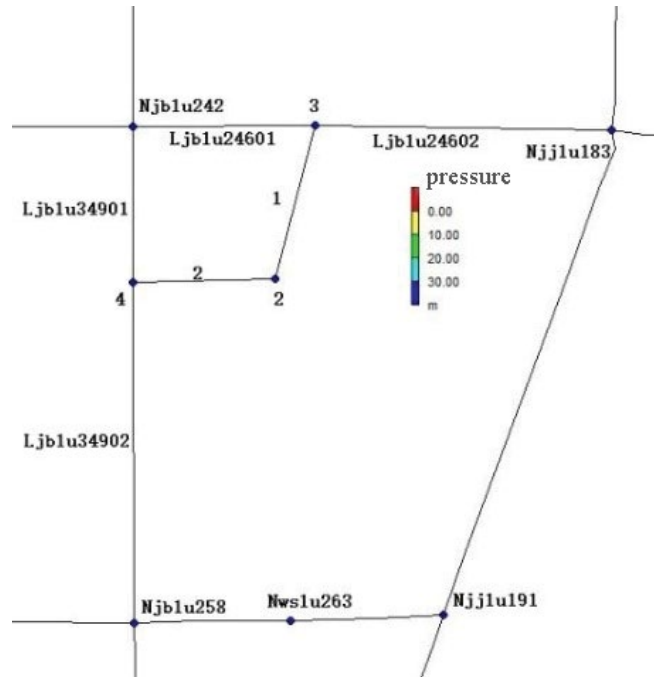


Fig. 2. Regional simulation of ANPF.

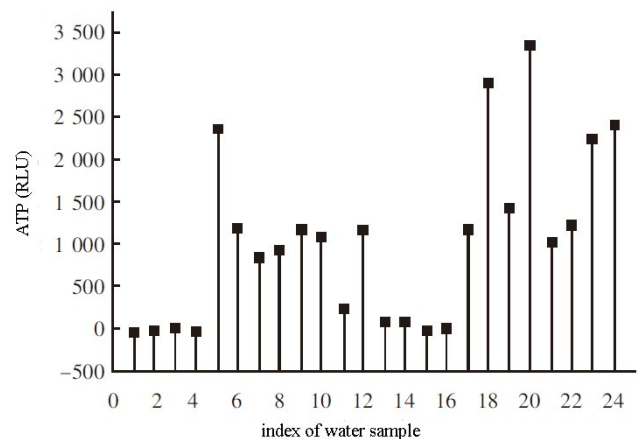


Fig. 3. ATP of water sample.

Integrating ANPF and composite disinfection technology, the integrating intelligent water management software includes system management, comprehensive data query, equipment management, equipment repairment, equipment inspection, access control management and supervisory control and data acquisition (SCADA). In the background of the smart water, the integrating intelligence water management software makes the management of SWS intellectual, standardized, technical, humanized and ecological.

The system management module is designed for the setting of function and parameter of SWS. This module provides a basis for all the other modules. The comprehensive data query module is designed for minimizing the coupling of infrastructure and coping with the trend in server development such as cloud computing, virtualization, centralization, and high density. The equipment management, equipment

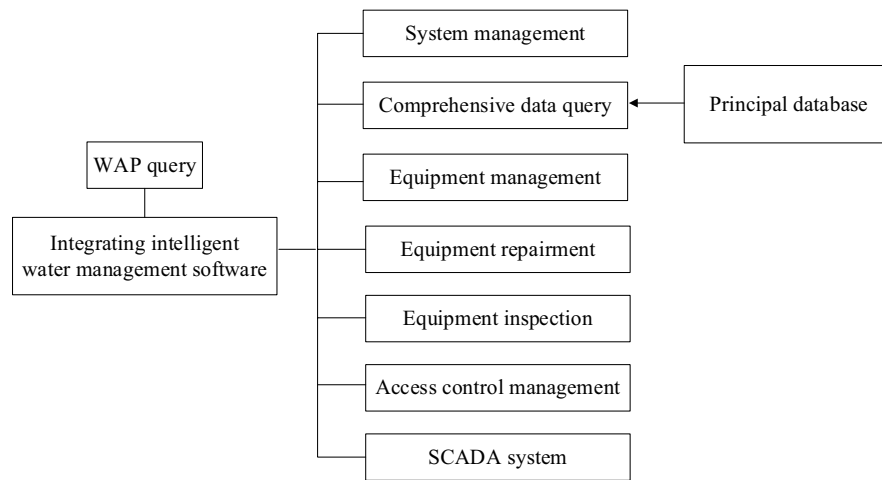


Fig. 4. Constitution of integrating intelligence water management software.

repairment, equipment inspection, and access control management module are designed for better operational status of SWS equipment. As a computer-based production process control and dispatch automation system, SCADA can monitor and control the operational equipment. The architecture of SCADA system includes two parts. First, the front-end equipment is composed of the sensor, programmable remote transmission unit, communicating module of 4G LTE, display interface of secondary development, and related electrical devices. Second, back-end equipment is a cloud computing center. The cloud computing center comprises of web server, real-time database server, and historical database server. Thus, the real-time display and command control of the SWS system is realized.

### 3. Results and discussion

#### 3.1. Simulation results of ANPF

Table 1 shows the simulation of ANPF in different situations. The pipeline 1 and pipeline 2 are set the same parameters. The diameter is 100 mm. The friction coefficient is 110. The length is 100 m. The operating status is open. Node 2, node 3, and node 4 are also set the same parameter. The elevation is 7.5 m. The pressure is 41.297 m. The initial water flow is 0 L/s.

Two scenarios are simulated. One is a bilateral pipeline with a 100 mm diameter. The other is a unilateral pipeline

with a 100 mm diameter. The high pressure and low pressure are considered simultaneously.

Fig. 5 shows the relation between water pressure and water flow of node 2 in a bilateral pipeline with 100 mm diameter at high pressure. The water pressure is 41.30 m, when water flow is 0 L/s. The water flow is 88 L/s, when water pressure is 0 m. The water pressure decreases when the water flow increases. The relation between water pressure and water flow is a quadratic function.

Fig. 6 shows the constitution of the inlet water flow of node 2 in a bilateral pipeline with a 100 mm diameter at high pressure. In the beginning, all of water flow enters node 2 via pipeline 2. Until the water flow of node 2 at 1.3 L/s, the water flow of pipeline 1 starts to flow into node 2. Until the water flow of node 2 at 77.3 L/s, the water flow of pipeline 1 starts to be slightly larger than pipeline 2's. Before that, the water flow of pipeline 1 is smaller than pipeline 2's.

Fig. 7 shows the relation between water pressure drop and water flow of bilateral pipeline with 100 mm diameter under high pressure. Pipeline 2 firstly supplies water for node 2. This causes the water pressure of node 3 and node 4 of pipeline 2 upstream decreases. The maximum water pressure drop of node 3 and node 4 are 1.155 and 1.226 m, respectively. When the water pressure of ANPF inlet pipeline approaches to 0, the connection of main pipeline network reaches maximum water pressure decreases 1.226 m. Node 3 and node 4 located at the same partition of water

Table 1  
Simulation results of ANPF

Pipeline information					Node information				
Pipeline	Diameter (mm)	$C_{H-W}$	Length (m)	Status	Node	Elevation (m)	$H$ (m)	$Q_i^{avl}$ (L/s)	
1	100	110	100	Open	2	7.5	41.30	0	
2	100	110	100	Open	3	7.5	41.30	0	
Ljblu24601	600	105	100	Open	4	7.5	41.30	0	
Ljblu24602	600	105	182.30	Open	Njblu242	7.6	41.24	9.995	
Ljblu34901	300	105	100	Open	Njblu258	7.3	41.41	8.365	
Ljblu34902	300	105	193.82	Open	Njlu183	5.9	42.62	10.912	

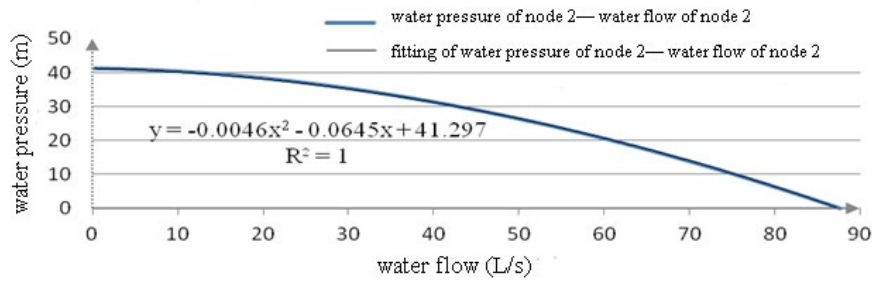


Fig. 5. Relation between water pressure and water flow under high pressure.

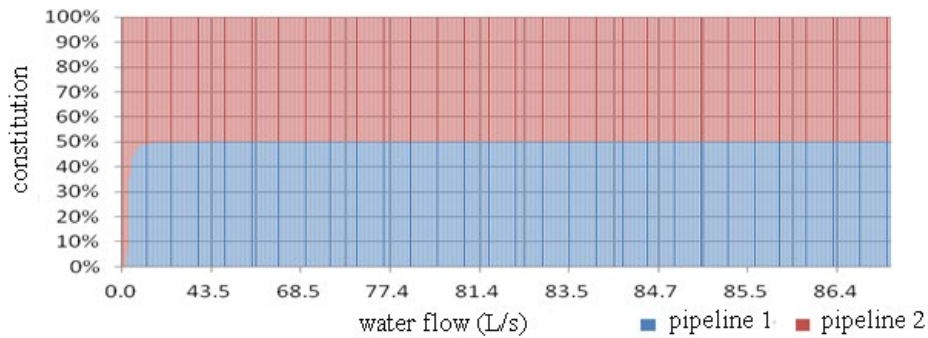


Fig. 6. Constitution of inlet water flow of node 2.

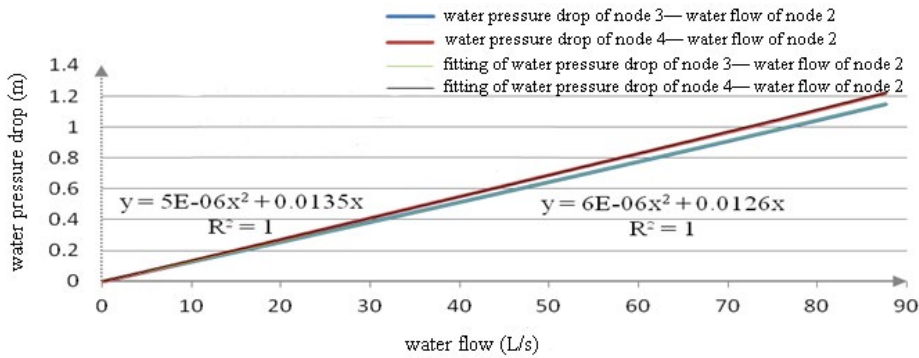


Fig. 7. Relation between water pressure drop and water flow under high pressure.

supply, leading to the decline of water pressure drop of node 3 and node 4.

Table 2 shows the initial setting of pipeline network information with pipeline 1, pipeline 2, node 2, node 3 and node 4.

The conditions of ordinary high pressure and ordinary pressure are also conducted, which are shown in Fig. 8. It can be seen that the water pressure drops under high pressure, ordinary high pressure and ordinary pressure are all 21.23 m when the water flow of node 2 is 30.76 L/s. The results reveal that the water pressure drop of the connection of main pipeline network is related to the maximum water flow of node 2, and is dependent on the water pressure of connection.

### 3.2. Optimization of ANPF

Conclusions can be drawn from the simulation results of ANPF:

- If the main pipeline has enough water supply and the access pipeline has a larger diameter, it will be suitable for ANPF. Meanwhile, limiting the water flow is critical to ensure normal water supply in the main pipeline with ANPF.
- The maximum water supply of ANPF is related to the water pressure of the connection of the main pipeline, a diameter of main pipeline, and diameter, length, and a number of access pipelines.
- The inlet water pressure is related to the water pressure and water flow of the connection, and the diameter and length of the access pipeline.

Based on the experimental comparisons on six pipeline networks, it is found that the ANPF has a degree of applicability considering the real conditions in Suzhou, China. However, the ANPF will stop the water supply, if

Table 2  
Initial setting of pipeline network information

Pipeline information				Node information			
Pipeline	Diameter (mm)	Length	Status	Node	Elevation (m)	H (m)	$Q_i^{avl}$ (L/s)
1	100	100	Open	2	17.5/27.5	31.23/21.23	0
2	100	100	Close	3	17.5/27.5	31.23/21.23	0
				4	17.5/27.5	31.30/21.30	0

there is a power outage or pipeline network malfunctions. Furthermore, at the peak of the water supply, if the water pressure becomes insufficient because of the ANPF connection to main pipeline, it will affect household water consumption. Considering the disadvantages of ANPF, an

optimization scheme of ANPF with a water tank pressure boost is proposed in this work. First, the import pipeline directly connects to the main pipeline. The water delivered to the lower level water tank. Meanwhile, a liquid level controller before the main pipeline is adopted to import to a

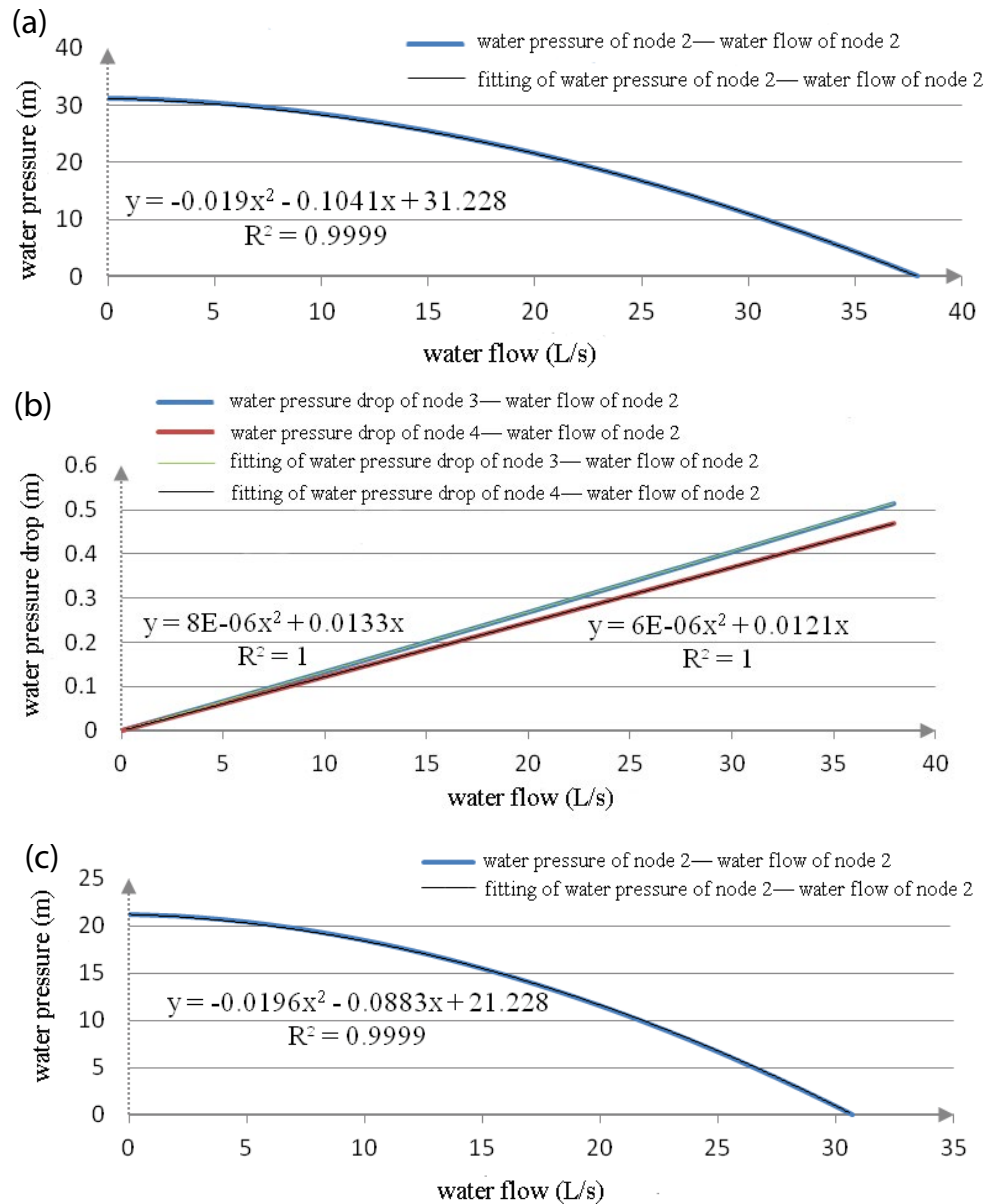


Fig. 8. Continued

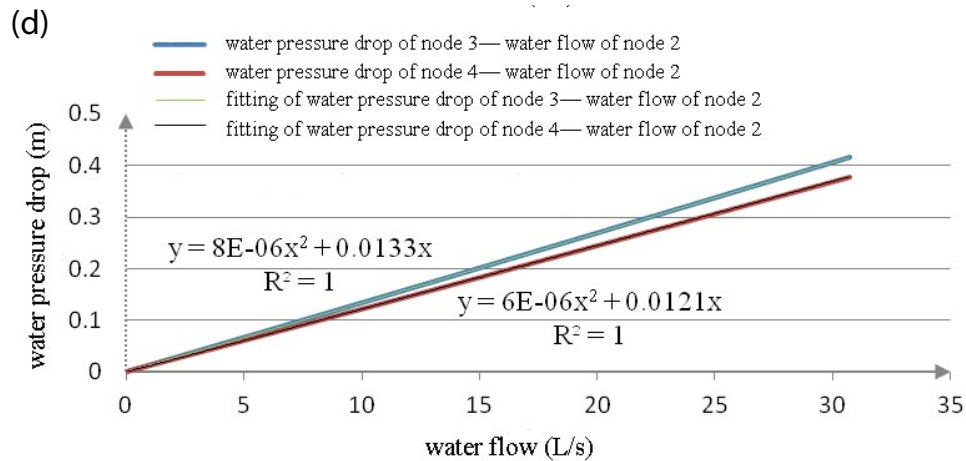


Fig. 8. (a) Relation between water pressure and water flow under ordinary high pressure, (b) relation between water pressure drop and water flow under ordinary high pressure, (c) relation between water pressure and water flow under ordinary pressure, and (d) relation between water pressure drop and water flow under ordinary pressure.

residential district. After that, according to the specific situation of water supply, water is transmitted to the households by pressurization or by pressurization combined with a variable frequency pump. Fig. 9 shows the optimization scheme of ANPF with a water tank pressure boost.

To avoid long hydraulic retention time, the following practices are used to optimize ANPF with a water tank pressure boost:

- Standardization of water tank. The firewater and domestic water are separated. The overflow pipeline and drain pipeline are separated. The water tank is locked for preventing external pollution sources.
- Constant water level. The water level fluctuation of the water tank is harmful to the water supply of SWS. Maintaining a constant water level can effectively reduce the water pressure fluctuation of the SWS and increase the minimum pressure of the water supply network.
- Optimal adjustment of variable frequency pump. The optimal adjustment of the variable frequency pump can

make a good trade-off of energy-saving and safety of water supply.

### 3.3. Results of terminal disinfection technology

Fig. 10 shows that the ATP intensity and volume in *Escherichia coli* liquid medium have a good positive linear relation. The standard variance is 0.92. The slope is 3.7. Therefore, ATP can be used to describe the bacteria in the liquid.

Fig. 11 shows the effects of UV disinfection, NaClO disinfection, and UV-NaClO disinfection. When the water sample is disinfected by NaClO, the number of bacteria colonies decreases significantly. The ATP intensity decreases from 102–202 RLU to 69–134 RLU. This result indicates that the disinfection only by NaClO has a positive effect. The effect of NaClO disinfection is nearly the same as UV-NaClO disinfection. The ATP intensity of NaClO disinfection is 69–134 RLU. The ATP intensity of UV-NaClO disinfection is 72–130 RLU. The water sample disinfected by NaClO

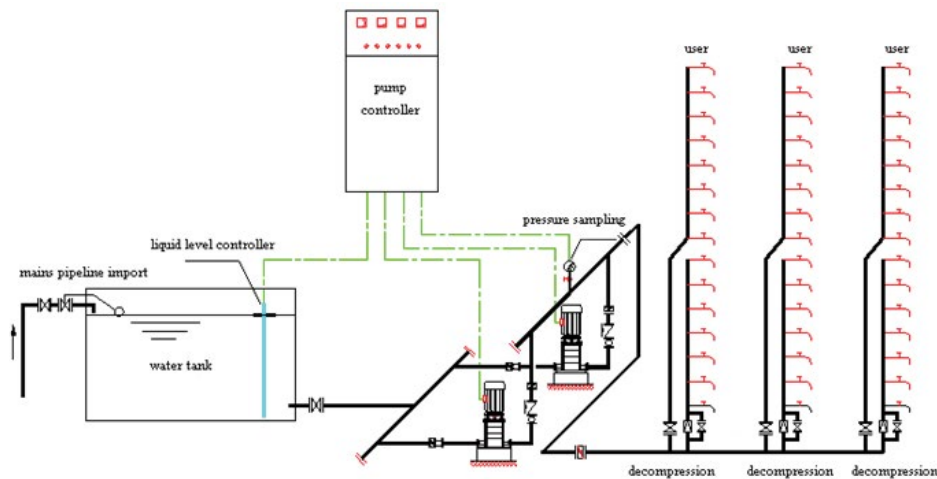


Fig. 9. Optimization scheme of ANPF with a water tank pressure boost.

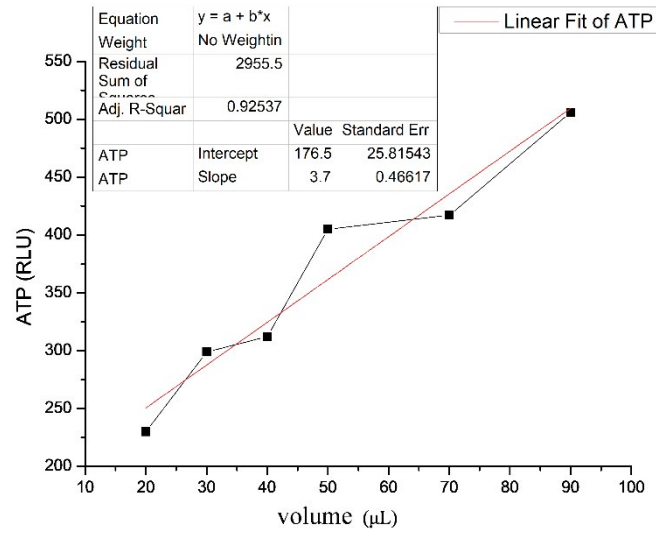


Fig. 10. Relation between ATP intensity and volume in *Escherichia coli* liquid medium.

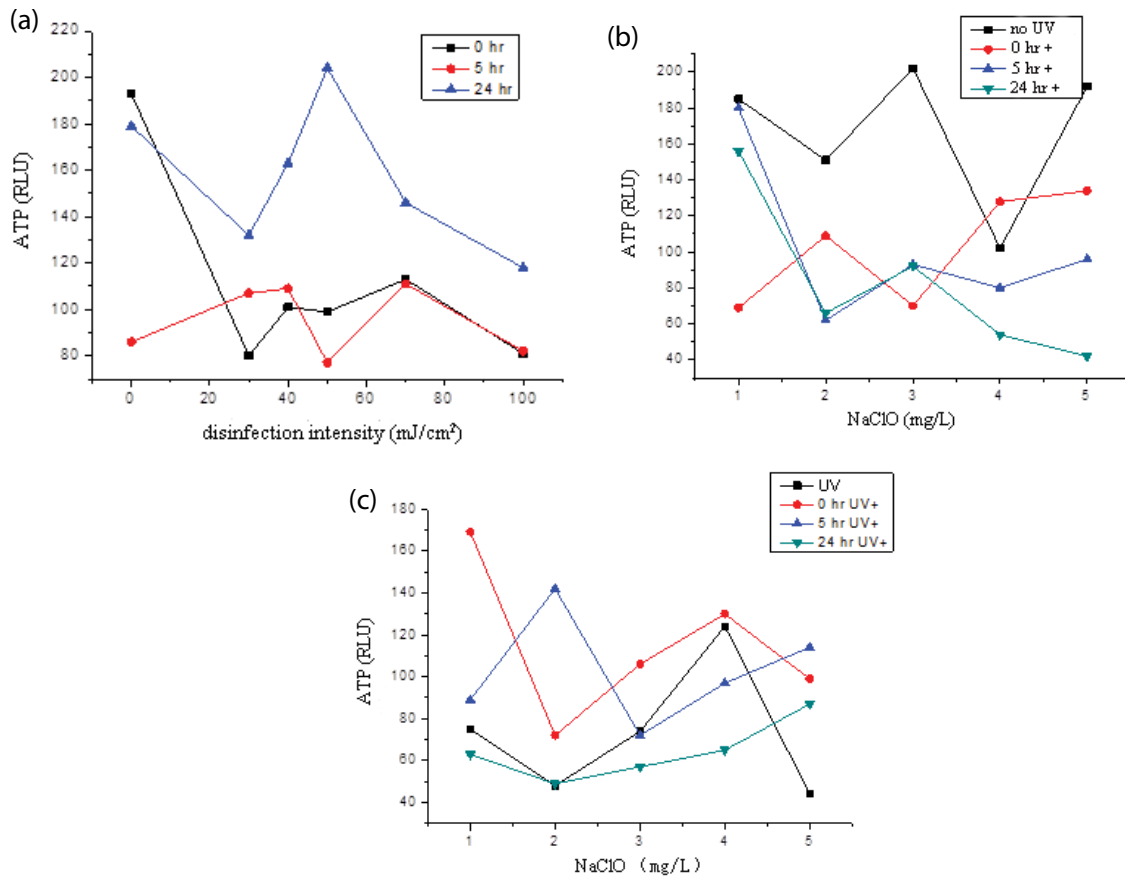


Fig. 11. Effects of (a) UV, (b) NaClO, and (c) UV-NaClO disinfection.

disinfection in 5 and 24 h is nearly the same as UV-NaClO disinfection. Furthermore, these two disinfection methods with a capacity of bacteria regrowth have no obvious difference, even cultivated at 24 h and in 38°C.

To further study the capacity of bacteria regrowth after disinfection, the water sample has been disinfected by NaClO

after it is disinfected by UV disinfection. Fig. 12 shows a flow chart of UV disinfection on water bio-indices stability of water. The collected water sample is divided into two parts. One part is added 2 mg/L NaClO, and the other part is not. Fig. 13 shows the ATP intensity of UV disinfection and UV-NaClO disinfection in 18°C, 28°C, and 38°C, respectively.

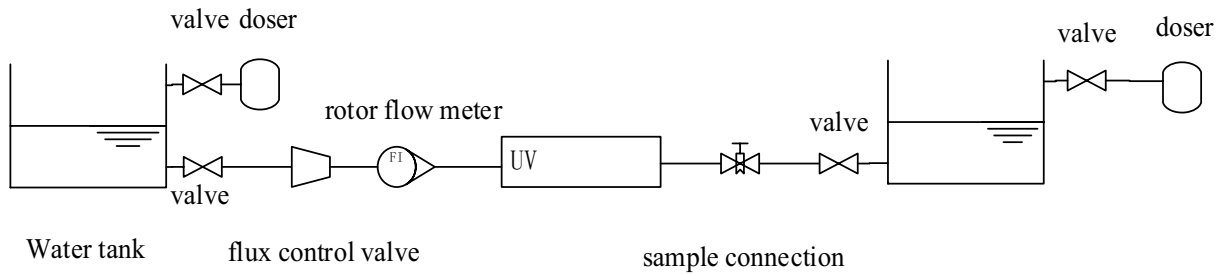


Fig. 12. Flow chart of UV disinfection.

Fig. 13a shows that the ATP intensity of UV disinfection is far less than 200 RLU in 18°C. It proves that low temperature is unfavorable to the regrowth of bacteria. The UV disinfection effect in 18°C satisfies the national safety standard of bacterial colonies.

Fig. 13b shows that the ATP intensity of UV-NaClO disinfection is less than 200 RLU in 28°C. The UV-NaClO disinfection effect basically satisfies the national safety standard of bacterial colonies. However, the ATP intensity of some water samples is greater than 200 RLU. The bacterial colonies of water sample approach the national standards upper limit. Therefore, UV-NaClO disinfection is required in 28°C.

Fig. 13c shows that the ATP intensity of UV disinfection is less than 100 RLU within 12 h in 38°C. However, the ATP intensity is greater than 200 RLU after 24 h. Bacteria regrows and the risk of bacteria exceeding the standard is increasing. This result shows that it is necessary to use UV-NaClO disinfection. Bacteria regrowth can be effectively prevented when the effective chlorine concentration is 2 mg/L.

Fig. 14 shows the bacterial growth effect of UV disinfection using the dilution cultivation method. Fig. 14a shows the growth effect with no UV disinfection. Fig. 14b shows the growth effect with 40 mJ/cm<sup>2</sup> UV disinfection. Fig. 14c shows the growth effect with 100 mJ/cm<sup>2</sup> UV disinfection. The results indicate that bio-indices stability is within the critical

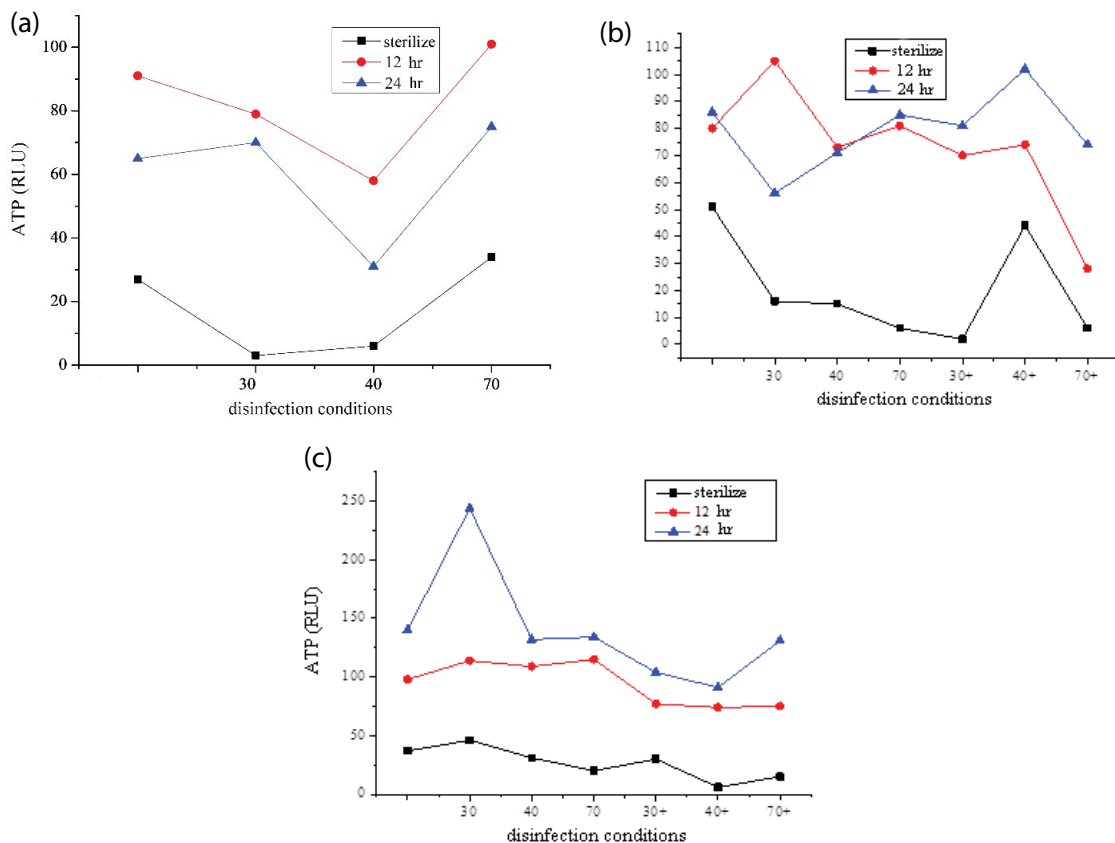


Fig. 13. ATP intensity in (a) 18°C, (b) 28°C, and (c) 38°C.

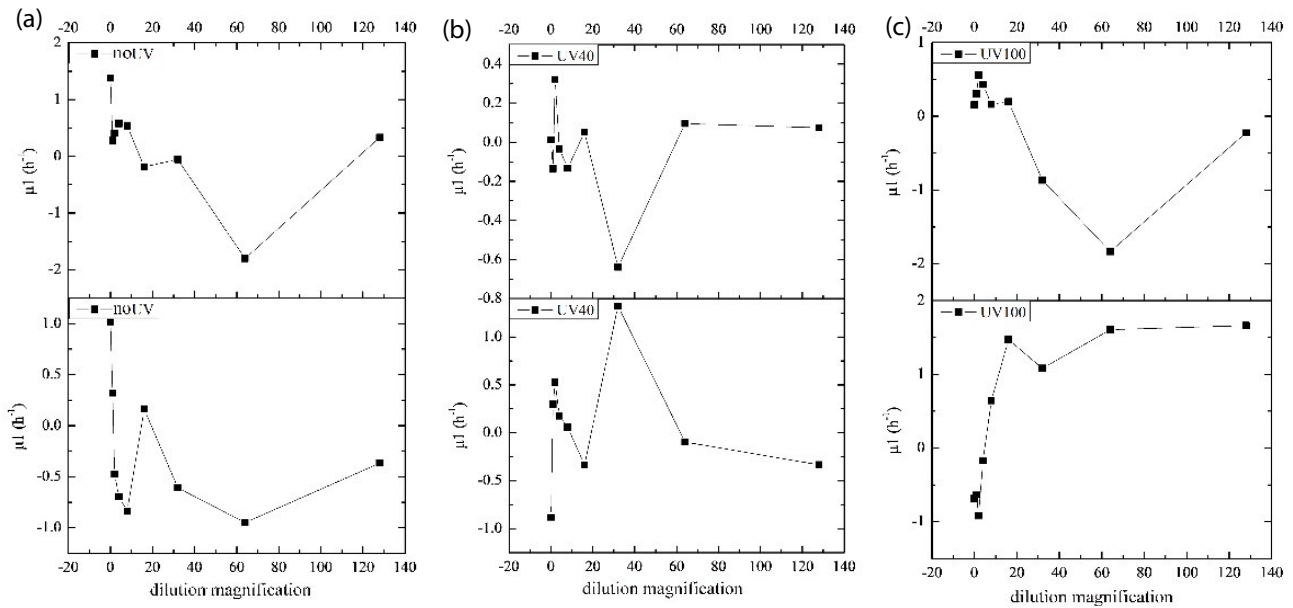


Fig. 14. Bacterial growth effect with (a) no, (b) 40 mJ/cm<sup>2</sup>, and (c) 100 mJ/cm<sup>2</sup> UV disinfection.

concentration. The effect of disinfection on bio-indices stability is not obvious.

3.4. Dual monitoring scheme of bio-indices stability

A dual monitoring scheme of bio-indices stability is proposed in this work by analyzing the disinfection effects with different UV intensity. As shown in Fig. 15, rapid monitoring and routine monitoring are conducted respectively. It makes up for the lack of water bio-indices stability and the timeliness in routine monitoring. The proposed dual monitoring scheme is beneficial for the flexible management of UV disinfection. The preliminary results, including existing biomass and acetate carbon, are obtained within

2–3 h. If the result of rapid monitoring or routine monitoring is unqualified, the disinfection equipment is then started in time.

4. Discussion

With the use of an optimization scheme of ANPF with a water tank pressure boost, the energy consumption is reduced by taking full advantage of the main pipeline pressure. Applied results show that the fluctuation of water pressure is controlled within 0.03 MPa. Fig. 16 shows the water pressure fluctuation in 16:00 to 18:00 at the peak time of water supply. Because the rooftop water tank is replaced, the water transmitted to the households remains fresh.

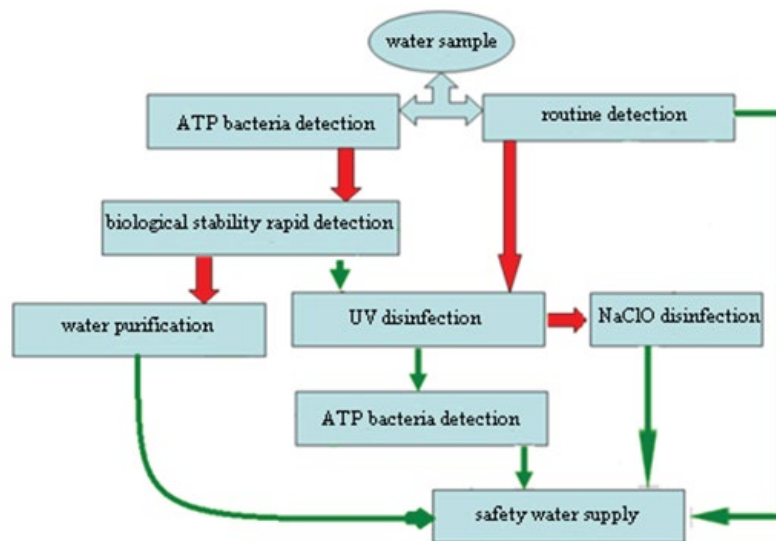


Fig. 15. Monitoring scheme of water bio-indices stability.

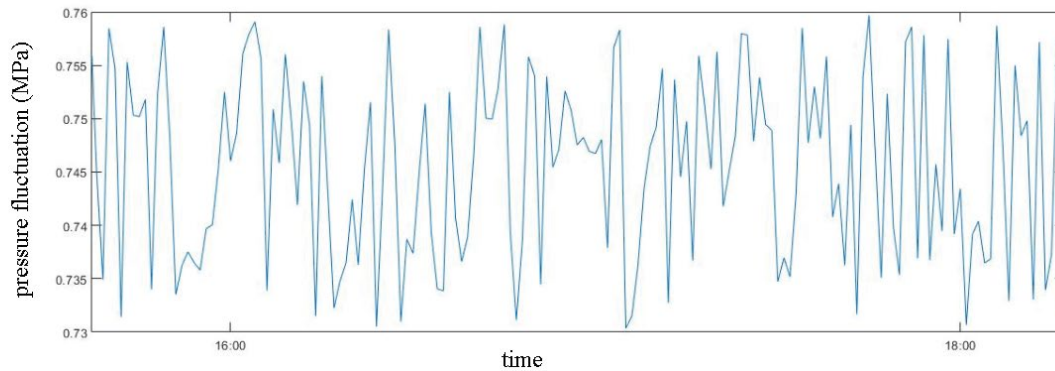


Fig. 16. Water pressure fluctuation.

Considering the difference in water temperature in all seasons, the UV- $\text{NaClO}$  disinfection technique is adopted. To intuitively track the difference of water quality between before and after SWS transformation, 20 continuous monitoring points of tap water quality are selected over a period of 6 months. Fig. 17 shows the distribution of these monitoring points. The monitoring point is determined according to the water age, the distribution of old and new communities, sample frequency, the detection index et al. Table 3 shows the water quality before SWS transformation. Table 4 shows the water quality after SWS transformation.

The implementation of SWS renovation project brings good social, environmental, and economic benefits to Suzhou, China. Besides that, the SWS reconstruction project helps energy conservation and emission reduction. It promotes the sustainable development of water resources.

### 5. Conclusions

This study develops the safety guarantee technologies of SWS of high-rise buildings. The optimization scheme of ANPF with a water tank pressure boost is proposed to

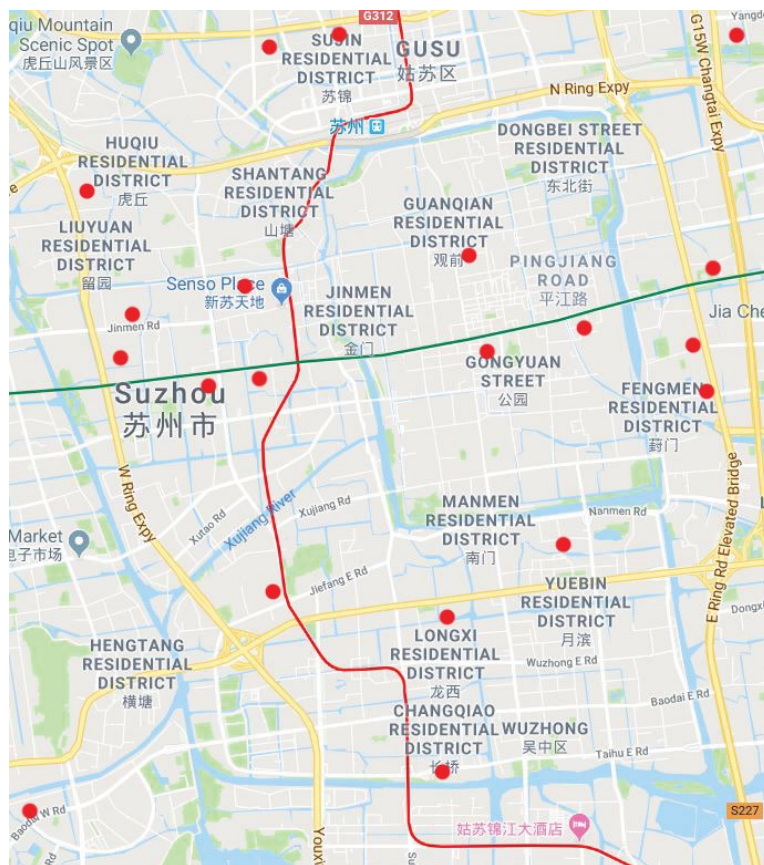


Fig. 17. Distribution of water quality monitoring points.

Table 3  
Water quality before SWS transformation

Order	Monitoring item	Maximum	Minimum	Limits	Qualification (%)
1	Turbidity (NTU)	5.2	0.21	≤1.0	68
2	Residual chlorine (mg/L)	0.46	0.02	≥0.05	86
3	Chroma	16	5	≤15	98
4	Visible	Rust particles	None	None	95
5	Taste and odor	Less mud	No detection	No detection	98
6	PH	9.8	7	6.5–8.5	98
7	Mn (mg/L)	0.41	0.05	≤0.1	96
8	Zn (mg/L)	2.36	0.02	≤1.0	98
9	Fe (mg/L)	0.95	0.05	≤0.3	89
10	Number of bacterial (CFU/mL)	83	0	≤100	100
11	Number of coliform (CFU/100 mL)	0	0	No detection	100
Water sample qualification		61%			

Table 4  
Water quality after SWS transformation

Order	Monitoring item	Maximum	Minimum	Limits	Qualification (%)
1	Turbidity (NTU)	0.7	0.05	≤1.0	100
2	Residual chlorine (mg/L)	0.5	0.05	≥0.05	100
3	Chroma	14	3	≤15	100
4	Visible	None	None	None	100
5	Taste and odor	No detection	No detection	No detection	100
6	PH	8	7	6.5–8.5	100
7	Mn (mg/L)	0.08	0.02	≤0.1	100
8	Zn (mg/L)	0.56	0.02	≤1.0	100
9	Fe (mg/L)	0.21	0.05	≤0.3	100
10	Number of bacterial (CFU/mL)	83	0	≤100	100
11	Number of coliform (CFU/100 mL)	0	0	no detection	100
Water sample qualification		100%			

stabilize the water pressure. The UV-NaClO disinfection is proposed to improve the water quality in terms of sensory properties and chemical index. The aforementioned technologies are successfully applied to a residential district in Suzhou, China. The results show that the qualified rate of water quality increases from 61% to 100%, and the water pressure fluctuates within 0.03 MPa.

### Acknowledgments

This work is supported by the National Natural Science Foundation of China (51708299), Science and Technology Project of Suzhou City (SS201803) and Science and Technology Project of Water Conservancy of Suzhou City (2018007).

### References

- [1] J. Du, H. Yang, Z. Shen, J. Chen, Micro hydro power generation from water supply system in high rise buildings using pump as turbines, *Energy*, 137 (2017) 431–440.
- [2] M. Li, Z. Qiang, J.R. Bolton, W. Li, P. Chen, UV disinfection of secondary water supply: online monitoring with micro-fluorescent silica detectors, *Chem. Eng. J.*, 255 (2014) 165–170.
- [3] X. Zhang, Y. Qi, Y. Wang, J. Wu, L. Lin, H. Peng, Y. Zhang, Effect of the tap water supply system on China's economy and energy consumption, and its emissions' impact, *Renewable Sustainable Energy Rev.*, 64 (2016) 660–671.
- [4] B. Swaffer, H. Abbott, B. King, V.D.L. Leon, P. Monis, Understanding human infectious, cryptosporidium, risk in drinking water supply catchments, *Water Res.*, 138 (2018) 282–292.
- [5] H.H. Wang, S.M. Liu, F.L. Meng, L. Bai, Investigation of the impact of anti-negative pressure facility on a water distribution system, *Appl. Mech. Mater.*, 316–317 (2013) 719–722.
- [6] H. Li, S. Li, W. Tang, Y. Yang, J. Zhao, S. Xia, H. Wang, Influence of secondary water supply systems on microbial community structure and opportunistic pathogen gene markers, *Water Res.*, 136 (2018) 160–168.
- [7] M. Boost, P. Cho, S. Lai, W.M. Sun, Detection of *Acanthamoeba* in tap water and contact lens cases using polymerase chain reaction, *Optometry Vision Sci.*, 85 (2008) 526–530.
- [8] A. Nescerecka, T. Juhna, F. Hammes, Identifying the underlying causes of biological instability in a full-scale drinking water supply system, *Water Res.*, 135 (2018) 11–21.
- [9] K.P. Zhou, W.H. Bi, Q.H. Zhang, X.H. Fu, G.Q. Wu, Influence of temperature and turbidity on water COD detection by UV absorption spectroscopy, *Optoelectron. Lett.*, 12 (2016) 461–464.

- [10] C. Li, G. Wang, Analysis of the water quality deterioration in secondary water-supply systems, *Adv. Comput. Sci. Res.*, 1 (2015) 120–123.
- [11] Q. Xu, Q. Chen, S. Qi, D. Cai, Improving water and energy metabolism efficiency in urban water supply system through pressure stabilization by optimal operation on water tanks, *Ecol. Inf.*, 26 (2015) 111–116.
- [12] I.B. Gomes, M. Simões, L.C. Simões, The effects of sodium hypochlorite against selected drinking water-isolated bacteria in planktonic and sessile states, *Sci. Total Environ.*, 565 (2016) 40–48.
- [13] S. Drakopoulou, S. Terzakis, M.S. Fountoulakis, D. Mantzavinos, T. Manios, Ultrasound-induced inactivation of gram-negative and gram-positive bacteria in secondary treated municipal wastewater, *Ultrason. Sonochem.*, 16 (2009) 629–634.
- [14] B.A. Brown-Elliott, R.J. Wallace, C. Tichindelean, J.C. Sarria, S. McNulty, R. Vasireddy, M. Loeffelholz, Five-year outbreak of community- and hospital-acquired *Mycobacterium porcinum* infections related to public water supplies, *J. Clin. Microbiol.*, 49 (2011) 4231–4238.
- [15] G. Hua, D.A. Reckhow, Comparison of disinfection byproduct formation from chlorine and alternative disinfectants, *Water Res.*, 41 (2007) 1667–1678.
- [16] M. Cho, J.H. Kim, J. Yoon, Investigating synergism during sequential inactivation of *Bacillus subtilis* spores with several disinfectants, *Water Res.*, 40 (2006) 2911–2920.
- [17] W. Li, M. Li, D. Wen, Z. Qiang, Development of economical-running strategy for multi-lamp UV disinfection reactors in secondary water supply systems with computational fluid dynamics simulations, *Chem. Eng. J.*, 343 (2018) 317–323.
- [18] M. Li, W. Li, Z. Qiang, E.R. Blatchley III, On-site determination and monitoring of real-time fluence delivery for an operating UV reactor based on a true fluence rate detector, *Environ. Sci. Technol.*, 51 (2017) 8094–8100.
- [19] Y.M. Tian, Y.J. Si, H. Li, M.F. Wu, Evaluation and optimization of secondary water supply system renovation, *J. Zhejiang Univ.-Sci. A*, 8 (2007) 1488–1494.
- [20] T.T. Tanyimboh, M. Tabesh, R. Burrows, Appraisal of source head methods for calculating reliability of water distribution networks, *J. Water Resour. Plann. Manage.*, 127 (2001) 206–213.